

Cooking Oil Mixed with Residential Wood Burning Particles: A Wintertime Indoor Air Quality Study

Published as part of ACS ES&T Air *special issues* “Indoor Chemistry in the Context of a Changing Climate” and “The ALPACA Project-Alaskan Layered Pollution and Chemical Analysis Project”.

Logan Forshee, Andrew L. Holen, Judy Wu, Karolina Cysneiros de Carvalho, Vanessa Selimovic, Ellis S. Robinson, Damien T. Ketcherside, Sukriti Kapur, Andrew P. Ault, Lu Hu, Brent J. Williams, Peter F. DeCarlo, and Kerri A. Pratt*

 Cite This: <https://doi.org/10.1021/acsestair.5c00156>

 Read Online

ACCESS |

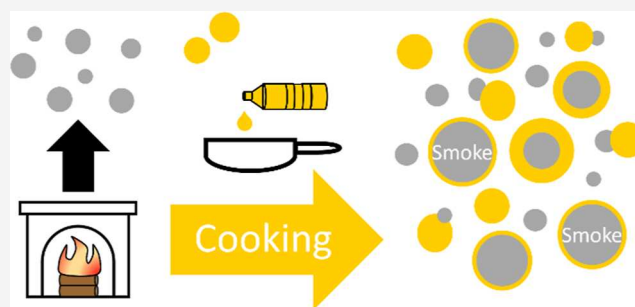
 Metrics & More

 Article Recommendations

 Supporting Information

ABSTRACT: Indoor air quality is important as humans spend significant time indoors, especially in colder climates. Household activities, including cooking and home heating, and infiltration of outdoor air contribute to gases and aerosols indoors. To study interactions of indoor aerosol sources, a single-particle mass spectrometer measured the size and chemical composition of individual aerosol particles inside a residential home in the winter in Fairbanks, Alaska. We focus on indoor measurements during nine cooking experiments, including five experiments with indoor home heating pellet stove burning. The three main single-particle types identified from the 70,384 individual particles (0.07–2 μm) measured during cooking were cooking oil-dominant, smoke (from indoor and infiltrated outdoor home heating), and smoke + cooking oil. Smoke + oil was the most abundant particle type (9–76%, by number, across the cooking experiments). Fatty acids and tocopherols from cooking oil were present in 71%, by number, of all measured particles during cooking. Indoor number mode diameters increased following cooking, supporting particle growth via coagulation of cooking oil particles with pre-existing wood smoke particles indoors and condensation of semivolatile cooking oil onto these particles. The physical mixing of smoke and cooking oil indoors demonstrates the interactions of aerosol sources in the indoor environment.

KEYWORDS: *single-particle, ATOFMS, fatty acids, tocopherols, smoke, pellet stove, cooking emissions*



1. INTRODUCTION

Discerning the factors that contribute to poor indoor air quality is crucial for evaluating adverse human health effects as people spend ~90% of their time indoors,¹ with increased time spent indoors when outdoor temperatures are low.² Despite this, fewer studies have investigated gas- and particle-phase pollutants indoors than outdoors.³ It is well-known that a major contributor to indoor aerosol particles is the infiltration of outdoor air,^{4–8} with less known about indoor emissions. Common indoor emission sources include cooking,^{9,10} cleaning,^{11,12} smoking and residual smoke,^{13–15} personal care products,¹⁶ building materials,¹⁷ and even humans.¹⁸ In many cases, the emitted gases and aerosol particles are poorly chemically characterized,¹⁹ and additional studies are needed. Characterizing indoor air is further complicated when considering the dynamics of infiltrating outdoor air through building leaks, windows, and doors, the continual re-equilibration of surface films, potential for reactive chemistry and gas/particle phase partitioning, and air removal processes

like HVAC (heating, ventilation, and air conditioning) filtration.^{20–23}

Understanding emissions indoors is crucial as indoor environments with human activities often have particulate matter (PM) concentrations that exceed those in the outdoor environment.^{24–26} Health-related impacts, including respiratory,²⁷ cardiovascular,²⁸ and neurological²⁹ issues, can occur when people are continually exposed to elevated levels of PM, particularly PM_{2.5} (PM with diameters less than 2.5 μm), due to its size-dependent ability to penetrate deeper into the lungs.³⁰ More specifically, previous studies have highlighted the potential health effects of cooking-related PM exposure.³¹

Received: April 30, 2025

Revised: November 15, 2025

Accepted: November 18, 2025

Table 1. Indoor Cooking Experiment Dates, Types, and Times during the ALPACA Field Campaign^a

date	experiment type	before experiment (AKST)	pellet stove burn (AKST)	cooking active (AKST)	decay (AKST)
01/29/22	pasta/sauce	6:00–9:00	N/A	12:03–13:00	13:00–14:55
01/29/22	oil aerosol generation 1	6:00–9:00	N/A	15:00–15:14	15:14–22:35
01/30/22	oil aerosol generation 2	N/A	N/A	13:15–13:30	N/A
01/30/22	pasta + chicken	10:02–12:02	N/A	15:00–16:13	16:13–21:12
02/07/22	mixed 1	7:22–10:22	10:22–13:02	12:22–12:40	13:02–19:21
02/08/22	mixed 2	N/A	9:15–11:45	11:13–11:27	N/A
02/09/22	mixed 3	7:15–10:15	10:15–12:45	12:15–12:30	12:45–20:01
02/10/22	mixed 4	8:30–11:30	11:30–14:02	13:21–13:43	14:02–21:14
02/16/22	mixed 5	11:48–15:00	15:00–17:58	16:47–17:07	17:58–23:58

^aActive cooking periods were defined by the duration the kitchen stove was on. Mixed experiments consisted of a pellet stove burning initially for ~120 min, after which frozen breaded chicken was fried in shallow soybean oil while the pellet stove was still burning. Due to instrument challenges, particle sizing data were not collected for the oil aerosol generation 2 or mixed 2 experiments. Before experiment periods are defined as 3 h, with deviations for the pasta + chicken and mixed 5 experiments based on data availability.

For example, Du et al.³² showed that 2 days of exposure to cooking emissions, notably, inhalable particles (PM₁₀; PM with diameters less than 10 μm), resulted in a significant reduction of lung function in healthy students. Additional studies have demonstrated that PM_{2.5} from cooking can decrease cell viability and induce oxidative stress,³³ which is further complicated by the presence of additional indoor emissions sources.^{34,35} Another consideration for the impact of cooking aerosol on indoors is that the majority of particles, by number, generated from cooking experiments are in the ultrafine range (i.e., below 100 nm),^{9,10} which have additional uncertain health impacts.³⁶

Cooking activities contribute an abundance of gas^{37–39} and particle emissions to the indoor environment.^{40–42} Previous studies have shown that cooking activities lead to significant increases in PM mass concentrations indoors,^{9,10,41,43} but the extent of this increase is highly variable across cooking techniques and conditions.⁹ The chemical composition of cooking-generated aerosol also depends on the ingredients, use of cooking oil, cooking style, and temperature.⁴⁴ Indoor cooking studies with bulk aerosol chemical composition measurements have found that cooking aerosol is primarily composed of organic aerosol, by mass.^{45,46} Brown et al.⁴⁵ found that fatty acids, carbohydrates, and phthalates generally dominate the organic aerosol population during cooking. This cooking aerosol also interacts with gases within the home, as shown by Lunderberg et al.,⁴⁷ who found that aerosols can uptake semivolatile phthalates, likely from vinyl flooring, post cooking. However, there have been few single-particle measurements investigating cooking aerosol chemical composition and its interactions with other gases and aerosols. In Beijing, China, Ma et al.⁴⁸ used single-particle mass spectrometry to identify individual cooking aerosol particles outdoors based on the presence of fatty acids, in addition to sulfate, nitrate, ammonium, and secondary organic compounds. However, to our knowledge, the chemical composition of individual indoor cooking aerosols has yet to be reported, thus limiting our current understanding of cooking-generated aerosol particles and their interactions with other indoor aerosols and gases.

Single-particle measurements can address the large uncertainty regarding contributions from various sources to the indoor aerosol population with the source-specific chemical identification of individual particles. For example, Dall'Osto et al.⁴⁹ used single-particle mass spectrometry of indoor air to identify the contributions of aerosol generated outdoors (e.g.,

dust) and indoors (e.g., tobacco smoke). In addition to the gap in understanding particles from indoor sources, the chemical reactions and physical mixing of particles and gases from indoor sources (e.g., cooking) and outdoor sources (e.g., vehicles) can uniquely transform both the size and chemical composition of indoor particles that are significantly understudied.

While indoor air environments are generally understudied,³ there is an even less known about indoor high-latitude environments,⁵⁰ despite residents spending more time indoors due to low temperatures and stricter cold-climate building codes making houses more airtight. Previous studies in wintertime Fairbanks, Alaska, have shown that a dominant source of outdoor aerosol particles is wood smoke, primarily from residential heating.^{51–53} However, it is not clear how these wood smoke particles, both in-home emissions and infiltrated outdoor emissions, interact in the home environment in the presence of emissions from indoor activities, including those generated during cooking.

During January–February 2022, the Alaskan Layered Pollution and Chemical Analysis (ALPACA) field campaign occurred in Fairbanks, Alaska, to study indoor and outdoor air quality in the cold environment.⁵⁴ In the present work, we investigate the size and chemical composition of individual aerosol particles generated during cooking inside a residential home and the interactions of cooking emissions with existing indoor particles, including pellet stove emissions. Three types of cooking experiments were conducted: heating cooking oil (2 experiments), boiling pasta and simmering pasta sauce (2 experiments), and shallow-frying breaded chicken (6 experiments). A home heating pellet stove was also burned indoors during five of the chicken-frying experiments to explore the potential interactions between these two emission sources. Individual particle size and chemical composition were measured indoors along with size-resolved particle number concentrations. Additionally, speciated semivolatile gas- and particle-phase measurements were used to quantify the contribution of cooking-oil-related species to both phases.

2. METHODS

2.1. Field Campaign and Particle Sampling. The ALPACA field campaign occurred in Fairbanks, AK, from January 17 to February 26, 2022.⁵⁴ An aerosol time-of-flight mass spectrometer (ATOFMS) (described in Section 2.2),^{55,56} a scanning mobility particle sizer spectrometer (SMPS, model 3082, TSI Inc.), an aerodynamic particle sizer (APS, model

3321, TSI Inc.), and a semivolatile thermal desorption aerosol gas chromatograph (SV-TAG) (described in the Supporting Information)^{57,58} were deployed in the attached garage of a residential home in Fairbanks.⁵⁴ For the ATOFMS and particle sizing instrumentation, air was continuously sampled through a computer-controlled inlet switcher,⁷ a Nafion dryer, and insulated copper tubing. The inlet switcher alternated sampling between outdoor and indoor air every 10 min; only the indoor data are investigated in the current work. The temperature inside the house remained constant at ~ 21 °C, and the house air exchange rate was estimated to be 0.19 air changes per hour during winter based on a blower door test at 50 Pa.⁵⁴ The house furnace air recirculation fan was continually operated with a MERV 4 filter for all experiments except for mixed 5 (Table 1), which had a MERV 8 filter.

The indoor sampling line to the inlet switcher was 10 m long (outer diameter (OD): 0.95 cm; inner diameter (ID): 0.79 cm), and the sampling lines from the inlet switcher to the SMPS, APS, and ATOFMS measured 1.8 m (OD: 0.64 cm; ID: 0.48 cm), 1.4 m (OD: 0.95 cm; ID: 0.79 cm), and 0.9 m (OD: 0.32 cm; ID: 0.17 cm), respectively. The flow rate and residence time from the inlet to the inlet switcher were 10 L min^{-1} and 3 s, respectively, and the flow rates and residence times from the inlet switcher to the SMPS, APS, and ATOFMS were 0.3 L min^{-1} and 6 s, 5 L min^{-1} and 0.8 s, and 0.07 L min^{-1} and 2 s, respectively. The SV-TAG collected particle- and gas-phase samples through a separate inlet that alternated between indoor and outdoor air, sampling hourly (described in the Supporting Information).

Several perturbation experiments were conducted within the residential home; we focus herein on nine experiments that involved cooking, as summarized in Table 1. The two cooking oil aerosol generation experiments were conducted by dropping approximately 20 drops of water into soybean oil (60 mL) that was heated on an electric stove at medium-high heat for 10 min. For the two pasta boil/sauce simmer experiments, pasta was added to salted boiling water and cooked as instructed on the box, after which the pasta sauce was simmered for 5 min at medium-low heat. After the pasta boil/sauce simmer, one of these two experiments also included shallow-frying frozen breaded chicken for 10 min in heated soybean oil (60 mL). Five “mixed” experiments consisted of shallow-frying frozen breaded chicken in heated soybean oil in the kitchen while a home heating pellet stove (Harman P35i) was burning in the living room. Note that the pellet stove leaked wood smoke emissions into the house for every mixed experiment due to a leak in the exhaust seal.⁵⁴ Reported cooking experiment times in Table 1 include background periods, the pellet stove burn time (for mixed experiments), and active cooking times. Background particle number concentrations were determined by examining SMPS and APS data for ~ 3 h, depending on data availability, prior to the experiment start. Decay periods were determined as the time from the end of active cooking to when particle number concentrations and mode diameters returned to the background (i.e., average levels before the experiment start). For the oil aerosol generation 1 and pasta + chicken experiments, the number mode diameters did not return to the average background levels, likely due to the influence of infiltrated outdoor air during the pollution event that occurred from Jan 29 to the afternoon of Feb 3;⁵⁴ therefore, the decay period conclusion was defined as after 30 min of stable particle

number concentration (defined as being within 1 standard deviation of the prior 3 h particle number concentration).

During all indoor cooking experiments with particle sizing data (Table 1), 96%, by number concentration, of the measured 0.013–16.5 μm d_m indoor aerosol was between 13 and 661 nm d_m . Therefore, only the SMPS size distributions (12.6–661.2 nm d_m for 5 min scans and 14.1–593.5 nm d_m for 2 min scans) for cooking experiments with particle sizing data are discussed herein.

2.2. Aerosol Measurements. The SMPS and APS measured size-resolved number concentrations of aerosol particles with 5 min resolution from January 26, 8:10 AKST to February 6, 22:00 AKST and with 2 min resolution for the remainder of the campaign. The SMPS measured particles from 12.6 to 661 nm in electrical mobility diameter (d_m). The APS measured particles from 0.523 to 19.81 μm in aerodynamic diameter (d_a). The SMPS and APS data were combined into a continuous size distribution from 0.01 to 16.5 μm d_m , similar to the method described by Khlystov et al.⁵⁹ For these calculations, we assume a shape factor of 1 and a density of 1.2 g cm^{-3} based on previous single-particle measurements of biomass burning aerosol,^{60,61} since the indoor aerosol population in this study primarily consisted of wood smoke aerosol, as described in Section 3.3. Due to instrument challenges during the campaign, SMPS and APS data were not obtained for the oil aerosol generation 2 experiment, and SMPS data were not obtained for the mixed 2 cooking experiment. The aerosol size distribution number mode diameters were found for each SMPS scan by fitting a log-normal curve to each size distribution using Igor Pro 8 (Wavemetrics).

An ATOFMS measured the size and chemical composition of individual aerosol particles from 0.07 to 2 μm in vacuum aerodynamic diameter (d_{va}) in real time.^{55,56} In brief, the ATOFMS uses an aerodynamic lens system that collimates aerosol particles into a narrow beam. Particles then enter a sizing region where they individually scatter the light from two continuous wave lasers (488 and 405 nm, OBIS, Coherent Inc.). From the time required to traverse these laser beams, particle speed is calculated and calibrated to d_{va} using 0.09–1.5 μm polystyrene latex spheres (Polysciences, Inc.) with a known density of 1 g cm^{-3} . Finally, particles enter a Z-configuration dual-polarity time-of-flight reflectron mass spectrometer (Tofwerk), where particles are individually desorbed and ionized by a 266 nm Nd:YAG laser (Centurion, Quantel, Inc.) to generate positive and negative ion mass spectra for each particle. ATOFMS mass spectra for 440,455 individual indoor particles were analyzed in the Flexible Analysis Toolkit for the exploration of SPMS data (FATES), a MATLAB (Mathworks, Inc.) toolkit created for analyzing ATOFMS data.⁶² The results herein focus on 70,384 individual particles that were measured during the nine cooking experiments.

From the 70,384 individual particles measured during all cooking experiments, single-particle mass spectra containing cooking oil (henceforth referred to as oil-containing particles) were identified based on the presence of at least one of the following ions: deprotonated linoleic acid ($\text{C}_{18}\text{H}_{31}\text{O}_2^-$, m/z -279), oleic acid ($\text{C}_{18}\text{H}_{33}\text{O}_2^-$, m/z -281), stearic acid ($\text{C}_{18}\text{H}_{35}\text{O}_2^-$, m/z -283), β - γ -tocopherol ($\text{C}_{28}\text{H}_{48}\text{O}_2^+$, m/z 416), or δ -tocopherol ($\text{C}_{27}\text{H}_{46}\text{O}_2^+$, m/z 402).^{63–65} These individual oil-containing particle mass spectra were further separated into three chemically distinct particle types: cooking oil-dominant, smoke + cooking oil, and ECOC + cooking oil.

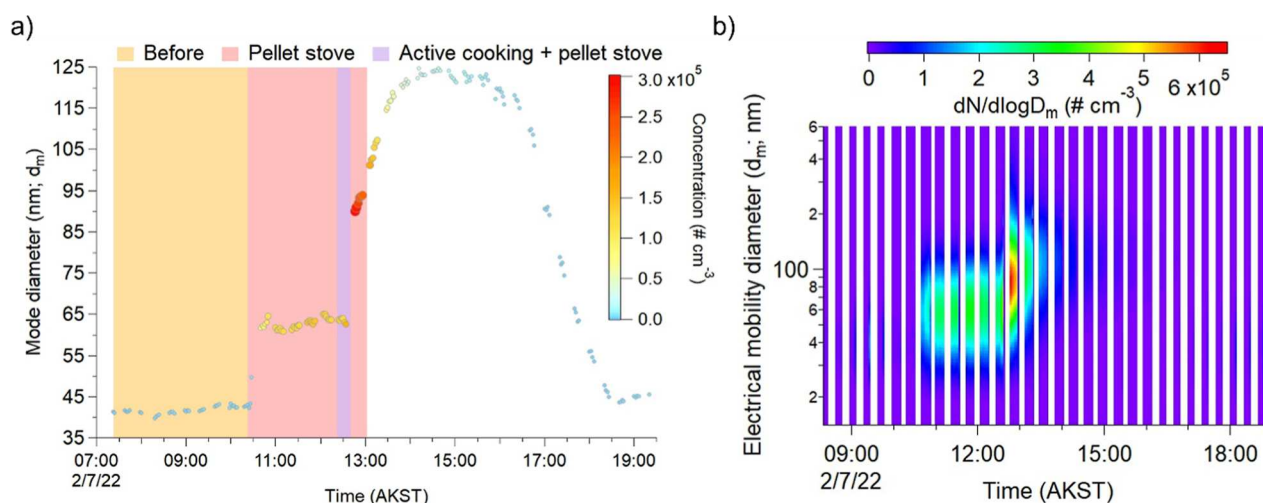


Figure 1. (a) Particle number mode diameters (d_m ; ranging from 14.1 to 593.5 nm) and particle number concentrations (particles cm^{-3} ; 0.01 – $16.5 \mu\text{m}$, d_m) from the combined APS and SMPS 2 min scans during the indoor mixed 1 (pellet stove + cooking) experiment. Particle mode diameters were found by fitting a log–normal distribution to each SMPS scan. Particle number concentrations are shown as a function of marker color and size, with larger markers representing higher number concentrations. The shaded background, pellet stove burn, and the continued pellet stove + active cooking periods were defined as 07:22–10:22 AKST, 10:22–13:02 AKST, and 12:22–12:40 AKST, respectively. Active cooking was defined by the time the kitchen stove was on. (b) Size-resolved aerosol number concentrations measured by the SMPS during the indoor mixed 1 (pellet stove + cooking) experiment. Time periods when the particle sizing instrumentation was sampling outdoor air are not shown.

ECOC + cooking oil particle mass spectra were distinguished from the other oil-containing particle types based on intense elemental carbon (C_n^+ , m/z 12, 24, 36, ...) and organic carbon (C_3H^+ , m/z 37) fragment ions relative to potassium (K^+ , m/z 39), a common ion marker used for wood smoke.^{66,67} Cooking oil-dominant particles were identified from the remaining oil-containing particles by a linoleic acid ion signal 10-fold higher than that of sulfate (HSO_4^- , m/z -97) and a β -/ γ -tocopherol ion signal higher than that of potassium. Both sulfate and potassium were selected for the ratios here because they are the dominant ions in the single-particle mass spectra of biomass burning aerosol.^{66–68} The remaining oil-containing particles were classified as smoke + cooking oil based on the dominance of potassium (K^+ , m/z 39) in the mass spectrum, plus elemental carbon (e.g., C_3^+ , m/z 36) and organic carbon fragment ions (e.g., C_3H^+ , m/z 37), consistent with the single-particle mass spectral signature of wood smoke.^{66–68} Examination of the variations in the grouped smoke + cooking oil mass spectra showed no evidence of additional contributing sources. The non-oil-containing particle type mass spectra (i.e., mass spectra that did not contain the fatty acid or tocopherol ions) were separated and identified as ECOC and smoke particle types based on the mass spectral signatures discussed above, but without the presence of the fatty acids or tocopherols. The ECOC mass spectra (with and without cooking oil) are consistent with prior single-particle mass spectrometry vehicle emission studies.^{69,70}

3. RESULTS

3.1. Increases in Particle Number Mode Diameters and Number Concentrations during Cooking Experiments. The average indoor aerosol number mode diameter during background periods, i.e., when no indoor experiment was being conducted, ranged from 41 to 50 nm (d_m). This is consistent with previous literature showing background indoor aerosol number mode diameters ranging from 28 to 69 nm in the absence of indoor activities.^{9,10,71} The indoor aerosol number mode diameter varied between experiments (Figures 1

and S1–S5), which we attribute to the complexity of factors influencing cooking-generated aerosol particles.⁴⁴

The mixed 1 experiment (Table 1) is discussed here in detail as an example as it produced 2–30-fold higher particle number concentrations than the other seven cooking experiments for which particle sizing data are available (Figures S1–S5). This high aerosol number concentration is likely due to the high heat applied during cooking that resulted in breaded chicken burning. Before the experiment began, the background aerosol showed an average number mode diameter of 41.8 ± 0.2 nm (Figure 1), within the range of the average background number mode diameters observed before the other cooking experiments (41–50 nm d_m). The mixed 1 experiment began with only home heating pellet stove burning. Compared to before the experiment began, the average number mode diameter and average aerosol number concentration increased to 65 ± 4 nm and $1.3 (\pm 0.2) \times 10^5$ particles cm^{-3} (from $3.1 (\pm 0.2) \times 10^3$ particles cm^{-3}), respectively, corresponding to a 56% increase in mode diameter and a 41-fold increase in particle number concentration, consistent with accumulation of pellet stove emissions indoors.⁵⁴ The average particle number mode diameter during the pellet stove burn was similar to the pellet stove burn mode diameters ranging from 55 to 91 nm d_m measured by Bari et al.⁷²

During the active cooking portion of the mixed 1 experiment, the aerosol particle number mode diameter and particle number concentration remained constant at ~ 64 nm and $\sim 1.3 \times 10^5$ particles cm^{-3} , respectively, likely due to the short duration of active cooking, which lasted 18 min and included ~ 5 min to heat the pan (Figure 1). The number mode diameter and particle number concentration spiked 6 min after the end of active cooking to 90.1 ± 0.3 nm and $3.0 (\pm 0.3) \times 10^5$ particles cm^{-3} , respectively, corresponding to increases of 41% and 131% compared to immediately before cooking began. This aerosol particle number mode diameter of 90.1 ± 0.3 nm is in agreement with previous literature showing a mode diameter of 89.8 nm for particles generated from heated soybean oil.⁷³ The particle number concentration (3.0

(± 0.3) $\times 10^5$ particles cm^{-3}) is also comparable to the 2018 HOMEChem study, where various cooking experiments exhibited average 4–100 nm diameter aerosol number concentrations of $1.5 (\pm 0.2) \times 10^4$ to $1.2 (\pm 0.5) \times 10^6$ particles cm^{-3} .⁹ Our study used an electric stove, similar to the electric hot plate that Patel et al.⁹ used when cooking stir fry vegetables. We measured a comparable number concentration of $1.1 (\pm 0.1) \times 10^4$ particles cm^{-3} for 14–20 nm particles to Patel et al.⁹ ($4 (\pm 2) \times 10^4$ particles cm^{-3}) at 52 min after cooking started. Therefore, it is likely that unmeasured particles less than 12.6 nm (d_m) may have been present in this study, as observed previously by Patel et al.⁹

After cooking ended during the mixed 1 experiment, the number mode diameter continued to increase to a maximum of 124.8 ± 0.6 nm, which occurred 92 min after the active cooking period of the mixed 1 experiment (Figure 1). This corresponds to a 39% increase in the number mode diameter and a 2.7-fold increase in the particle volume after cooking. For the initial 30 min after cooking ended, the calculated aerosol growth rate was 36 nm h^{-1} , which is higher than $\sim 28 \text{ nm h}^{-1}$ observed by Glytsos et al.⁷⁴ after onion frying. This 30 min period had an elevated average surface area concentration of $9.1 (\pm 0.9) \times 10^3 \mu\text{m}^2 \text{ cm}^{-3}$, compared to $1.2 (\pm 0.1) \times 10^2 \mu\text{m}^2 \text{ cm}^{-3}$ and $1.2 (\pm 0.1) \times 10^3 \mu\text{m}^2 \text{ cm}^{-3}$ before the mixed 1 experiment and during the mixed 1 experiment pellet stove burn, respectively. The elevated surface area concentration is comparable to previous indoor cooking aerosol literature, which have found average surface area concentrations ranging from 5.4 to $14.0 \times 10^4 \mu\text{m}^2 \text{ cm}^{-3}$ ⁴¹ and 6.8×10^2 to $1.9 \times 10^4 \mu\text{m}^2 \text{ cm}^{-3}$,⁴² and emphasizes the potential contribution of aerosol coagulation to particle growth.

During the 92 min period of the mixed 1 experiment that the number mode diameter took to reach its maximum after cooking ended, the particle number concentration decreased by 91% to $2.7 (\pm 0.3) \times 10^4$ particles cm^{-3} , which is 5-fold lower than the average number concentration ($1.3 (\pm 0.2) \times 10^5$ particles cm^{-3}) during the pellet stove burn but 9-fold higher than the average background number concentration (Figure 1). The decrease in particle number concentration is likely due to a combination of dilution of cooking aerosol from the kitchen into the rest of the house and aerosol deposition onto indoor surfaces as ultrafine particles are highly impacted by diffusional losses.⁷⁵ The decreasing particle number concentration may also be influenced by HVAC system filtration as a furnace fan continuously circulated air in the house. However, we expect this impact to be minimal as the furnace filters used in this study were MERV 4 and 8, both of which have low removal efficiencies (<20%) for ultrafine particles.⁷⁶ The simultaneously increasing particle number mode diameter and decreasing particle number concentration support contribution from aerosol coagulation. The calculated diameter of a particle formed from coagulation of a 65 nm pellet stove smoke particle (number mode diameter) and a 90 nm cooking oil particle (number mode diameter) is 100 nm, which is below the measured maximum number mode diameter of 124.8 ± 0.6 nm d_m in this study.

To further examine the contribution of coagulation to aerosol growth, we calculated the polydisperse aerosol coagulation coefficient after active cooking ended to be $1.4 \times 10^{-8} \text{ cm}^3 \text{ s}^{-1}$, which is similar to aerosol coagulation coefficients from previous indoor aerosol studies.^{77,78} We also calculated the theoretical number concentration and number mode diameter changes due to coagulation, which are

discussed in the Supporting Information and shown in Table S1. Overall, the increasing aerosol number mode diameter following active cooking is likely the result of polydisperse coagulation of cooking-generated aerosol, as well as semi-volatile cooking gases condensing onto the pre-existing indoor aerosol particles, likely primarily from the pellet stove emissions, as discussed in Section 3.2. After the particle number mode diameter reached a maximum, both the number mode diameter and number concentration decreased until they returned to background levels, ~ 45 nm and $\sim 3.6 \times 10^3$ particles cm^{-3} , respectively, consistent with particle losses from ventilation and deposition.

The mixed 1 experiment showed a trend of increasing number mode diameter and number concentration after cooking. However, this was just one experiment, and there can be significant variation in the aerosol population due to differences in cooking parameters (e.g., temperature, cooking style/method). Thus, the other six cooking experiments with SMPS and APS data were grouped by mixed experiments (pellet stove + cooking) or cooking-only experiments (i.e., pasta/Sauce, oil aerosol generation 1, pasta + chicken) for a more comprehensive evaluation of how these indoor activities influenced the aerosol size distributions. Similar to the average indoor number mode diameter (41.8 ± 0.2 nm) and average indoor number concentration ($2.4 (\pm 0.2) \times 10^3$ particles cm^{-3}) before the mixed 1 experiment, the average number mode diameter and number concentration before the other cooking experiments ranged from 41 to 50 nm and 8 to 30×10^2 particles cm^{-3} , respectively (Figures S1–S5). The variability in mode diameters and number concentrations before the cooking experiments was likely influenced by activity inside the house prior to the experiments in addition to variation in infiltrated outdoor aerosol.

The pellet stove burns for the other mixed experiments had average number mode diameters that ranged from 58 nm to 63 nm (Figures S3–S5), consistent with the average number mode diameter (65 ± 4 nm) during the mixed 1 experiment pellet stove burn. All seven cooking experiments with particle sizing data showed an increase in number mode diameter after active cooking compared to before cooking. For cooking-only (nonmixed) experiments, increases in the maximum number mode diameter after cooking compared to before ranged from 24% to 78%, with the wide range likely due to the different cooking ingredients/methods used in these experiments. For the other mixed experiments with aerosol size distribution data (mixed 3–5), the average number mode diameter during the pellet stove burn was already elevated compared to the background and then increased further by 25–46% after cooking, compared to a 49% increase for the mixed 1 experiment. The highest increase in number mode diameter after cooking during the mixed 1 experiment is likely due to elevated cooking emissions resulting from higher heat applied during this experiment than in the other mixed experiments (mixed 3–5). The maximum number mode diameter occurred between 1 and 55 min after cooking ended for the nonmixed experiments, compared to 127 min–139 min for the mixed 3–5 experiments, suggesting that semivolatile gases from the pellet stove burn likely were also condensing onto the particles during this time frame, thus resulting in prolonged aerosol growth.

Overall, the mixed 1 experiment resulted in the highest percentage increase in particle number mode diameter after cooking and produced the greatest particle number concen-

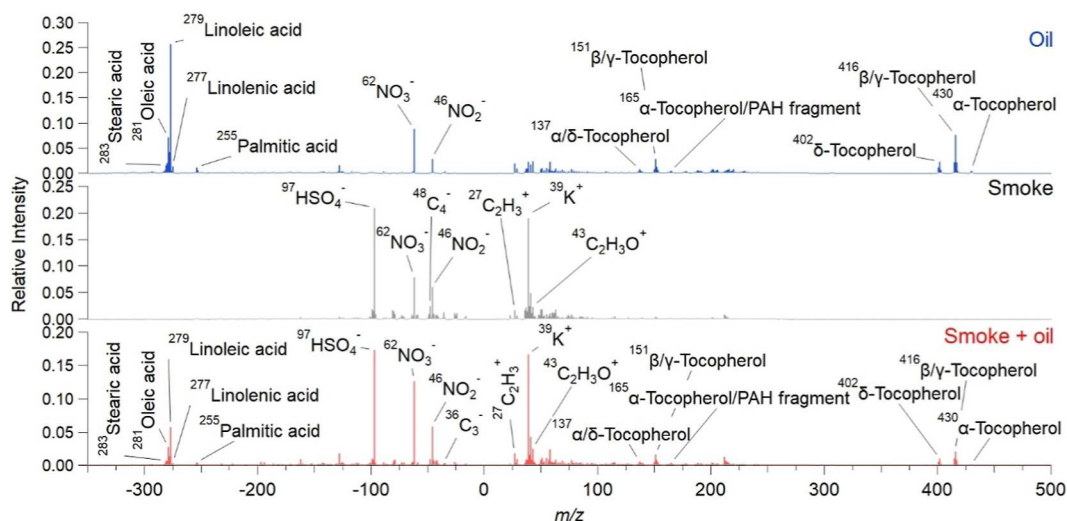


Figure 2. Average ATOFMS negative and positive ion mass spectra of the following single-particle types: cooking oil-dominant (top; 1764 particles), smoke (middle; 18,251 particles), and smoke + cooking oil (bottom; 45,566 particles), for all cooking experiments.

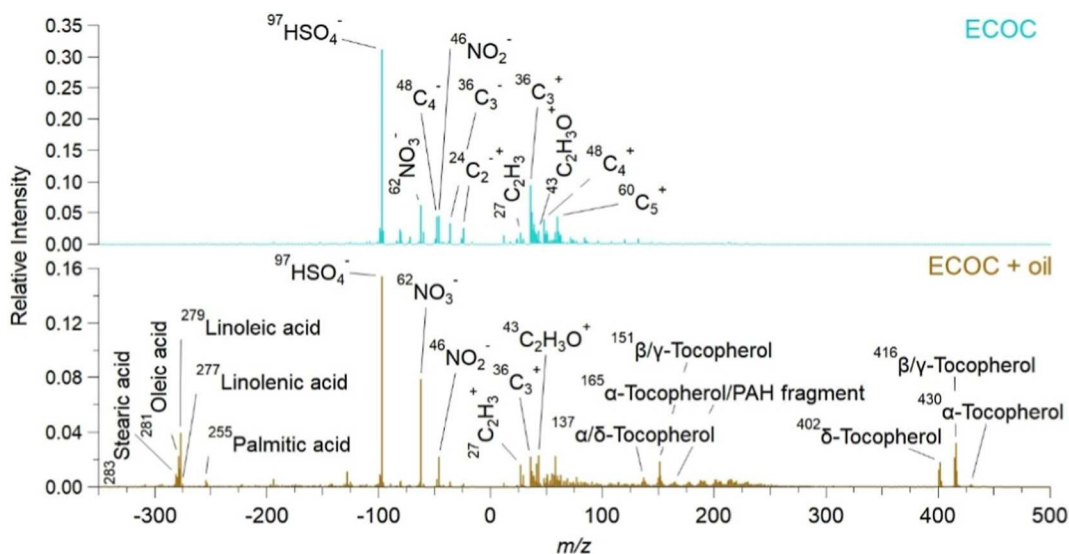


Figure 3. Average ATOFMS negative and positive ion mass spectra of the following single-particle types: ECOC (top; 1911 particles) and ECOC + cooking oil (bottom; 2892 particles) during all cooking experiments.

tration of all seven cooking experiments discussed above, likely due to burning the breaded chicken. The increase in particle mode diameter during all cooking experiments suggests the condensation of semivolatile gaseous cooking emissions onto pre-existing indoor aerosol particles and the coagulation of cooking-generated aerosol with indoor ambient aerosol. The decrease in the particle number concentration is likely from a combination of aerosol deposition to indoor surfaces, coagulation immediately following active cooking, and HVAC filtration. To further investigate the indoor aerosol particle population, we used single-particle mass spectrometry (i.e., ATOFMS) to chemically characterize individual aerosol particles during cooking experiments, as discussed in Section 3.2.

3.2. Single-Particle Measurements Show Mixtures of Wood Smoke + Cooking Oil within Individual Particles.

During the ALPACA campaign, the background indoor aerosol population (from 0.07 to 2 μm d_{va}) was mainly characterized by residential home heating particles that infiltrated from the

outdoor environment (Figure S6) as there was no indoor source of wood smoke during these times. During the active cooking and decay periods of the cooking experiments (Table 1), 70,384 individual particles (0.07–2 μm d_{va}) were measured by the ATOFMS (Figures S7–S9). Five different single-particle types were identified: cooking oil-dominant, smoke, smoke + cooking oil, elemental carbon/organic carbon (ECOC), and ECOC + cooking oil. The corresponding average mass spectra of these single-particle types are shown in Figures 2 and 3. This analysis focuses on three main particle types: oil-dominant ($2.47 \pm 0.06\%$, by number measured), smoke ($26.0 \pm 0.2\%$, by number), and smoke + oil ($64.8 \pm 0.2\%$, by number). ECOC, corresponding to infiltrated vehicle emissions, and ECOC + cooking oil particles comprised $2.72 \pm 0.06\%$ and $4.11 \pm 0.07\%$, by number, respectively, of the measured particles and are discussed briefly. Cooking oil was identified by the molecular ion peaks for β/γ -tocopherol ($\text{C}_{28}\text{H}_{46}\text{O}_2^+$, m/z 416) and linoleate ($\text{C}_{18}\text{H}_{31}\text{O}_2^-$, m/z -279),^{63,65} as described below. Particles containing both

wood smoke ion markers (discussed below) and cooking oil ion markers were classified as smoke + oil.

The average mass spectrum of cooking oil-dominant particles, shown in Figure 2, exhibits ions corresponding to deprotonated fatty acids commonly found in soybean oil: palmitic ($C_{16}H_{31}O_2^-$, m/z -255), linolenic ($C_{18}H_{29}O_2^-$, m/z -277), linoleic ($C_{18}H_{31}O_2^-$, m/z -279), oleic ($C_{18}H_{33}O_2^-$, m/z -281), and stearic ($C_{18}H_{35}O_2^-$, m/z -283) acids.⁷⁹ Molecular ions corresponding to deprotonated linoleic and oleic acids were observed in 100% and $51 \pm 1\%$, respectively, of the oil-dominant single-particle mass spectra, by number, while the other three fatty acids were observed in 13–19% of oil-dominant particles, by number. Vitamin E analogues α -tocopherol ($C_{29}H_{50}O_2^+$, m/z 430), β -/ γ -tocopherol ($C_{28}H_{48}O_2^+$, m/z 416), and δ -tocopherol ($C_{27}H_{46}O_2^+$, m/z 402) are also present in soybean oil⁷⁹ and were observed in $70 \pm 1\%$, 100%, and $25 \pm 1\%$ of the oil-dominant single-particle mass spectra, respectively. The average mass spectrum also shows tocopherol fragment ions $C_8H_9O_2^+/C_{10}H_{17}^+$ (m/z 137), $C_9H_{11}O_2^+$ (m/z 151), and $C_{10}H_{13}O_2^+$ (m/z 165) that have been identified in previous literature.^{63,64} Note that m/z 165 is also a common polycyclic aromatic hydrocarbon (PAH) fragment ion,⁸⁰ however, the relative intensity of m/z 165 is statistically higher ($p < 0.05$) in particles containing cooking oil markers when compared to background smoke aerosol (particles measured indoors when no experiment was occurring). Smoke aerosol generated from wood burning contains PAHs (e.g., naphthalene, acenaphthylene, pyrene),^{72,81} but smoke solely generated from burning wood would not contain cooking oil markers (e.g., tocopherols). This finding supports the identification of m/z 165 as a tocopherol fragment rather than a PAH fragment during the cooking experiments.

To support the ATOFMS measurements of soybean oil compounds in the particle phase, we report data from a Semi-Volatile Thermal Desorption Aerosol Gas Chromatograph (SV-TAG) that was deployed during the ALPACA field campaign to characterize and quantify both gas-phase and particle-phase compounds (methods described in the Supporting Information).^{57,58} During the mixed 1 and mixed 5 experiments, the SV-TAG quantified the particle-phase fractions (F_p) of four fatty acids (palmitic, linoleic, oleic, and stearic) and two mixed tocopherols (δ - and γ -tocopherol). F_p values ranged from 71% to 93% for the fatty acids and from 92% to 98% among the tocopherols (Figure S10). This demonstrates that these cooking oil-derived compounds, which were also measured by the ATOFMS within individual particles, do have the ability to transition phases but were primarily observed in the particle phase. The lower percentage of fatty acids than tocopherols in the particle phase also agrees with fatty acids being more volatile.^{82,83} The percentages of all six compounds in the particle phase were lower for the mixed 5 experiment (71–93%) than for the mixed 1 experiment (86–98%). The properties and chemical composition of cooking emissions depend on a number of factors, such as temperature, which could help explain the difference in F_p values during the mixed 1 experiment. The higher temperature used for the mixed 1 experiment led to burnt chicken, likely enabling greater volatilization of cooking oil compounds, which could then partition from the gas phase to the particle phase and result in an increased percentage of each compound in the condensed phase. The mixed 1 experiment also generated a larger number of larger particles, creating more particle mass

for the oil compounds to partition onto, a key parameter in phase partitioning dynamics.^{84,85} These SV-TAG measurements support the identification of cooking oil markers in the single-particle ATOFMS mass spectra during the cooking experiments.

Residential wood burning smoke particles were identified indoors by single-particle mass spectra with intense ion peaks corresponding to potassium (K^+ , m/z 39), elemental carbon (C_n^+ , m/z 12, 24, 36, ...), and organic carbon (e.g., $C_2H_3^+$, m/z 27) (Figure 2).^{66–68} Another prominent ion marker in the average mass spectrum of smoke particles corresponds to sulfate (HSO_4^- , m/z -97),⁸⁶ which has previously been observed in wood smoke particles.^{66,67,87,88} The indoor aerosol population during periods of no indoor perturbation experiment was primarily composed of wood smoke particles (Figure S6), and these particles were similar in composition to the pellet smoke particles measured during the mixed experiments (Figure 2). Therefore, in this study, smoke particles generated from the indoor pellet stove could not be chemically distinguished from infiltrated outdoor residential home heating particles. However, given the observed large aerosol number concentration increase upon the start of the pellet stove burns (Section 3.1), these pellet stove smoke particles are expected to be in much greater abundance than the infiltrated outdoor smoke, even within the ATOFMS size range. A subset ($30.8 \pm 0.3\%$) of the smoke particles measured indoors contained levoglucosan ($C_3H_3O_2^-$, m/z -71; $C_2H_3O_2^-$, m/z -59; CHO_2^- , m/z -45),^{86,89,90} a marker of fresh wood burning.⁹¹ Levoglucosan rapidly degrades in the atmosphere;^{92,93} however, the loss rates indoors and in Fairbanks during winter are unknown. It is worth noting that levoglucosan is not observed in all types of wood,⁹⁴ all biomass burning particles,^{66,92} or all stages of combustion,⁸⁸ so this suggests that the contribution of fresh wood burning to the measured indoor smoke is expected to be a lower limit.

The house used in this study was located in a residential neighborhood where many nearby residents use residential wood combustion (e.g., pellet stoves) to heat their homes.⁵⁴ In addition to infiltrated wood smoke, the indoor aerosol population is also influenced by the infiltration of other forms of residential heating (e.g., home heating oil combustion) emissions, as well as vehicle emissions, discussed below. However, the majority of particles measured during indoor background periods have a chemical composition similar to that of wood smoke (Figure S6) and are therefore classified as such. Another indication that the indoor aerosol particle population was largely influenced by infiltration of outdoor wood smoke is through the presence of secondary aerosol compounds within the background particles. For example, the oxygenated organic fragment ion ($C_2H_3O^+$, m/z 43), indicative of secondary organic aerosol,⁹⁵ was observed in $95.21 \pm 0.04\%$ of the smoke particles observed indoors during background periods (Figure S6). Similarly, oxalate ($HC_2O_4^-$, m/z -89),⁹⁶ formed through aqueous-phase reactions, was observed in $43.13 \pm 0.09\%$ of the infiltrated smoke particles. An additional indicator of infiltration of particles indoors from outside the house is the presence of ECOC particle types, indicative of vehicle combustion.^{69,97} The majority of the ECOC particles, described below, also contained oxygenated organics ($C_2H_3O^+$, m/z 43), indicative of atmospheric processing. These high number fractions of background indoor aerosol particles containing secondary aerosol species further

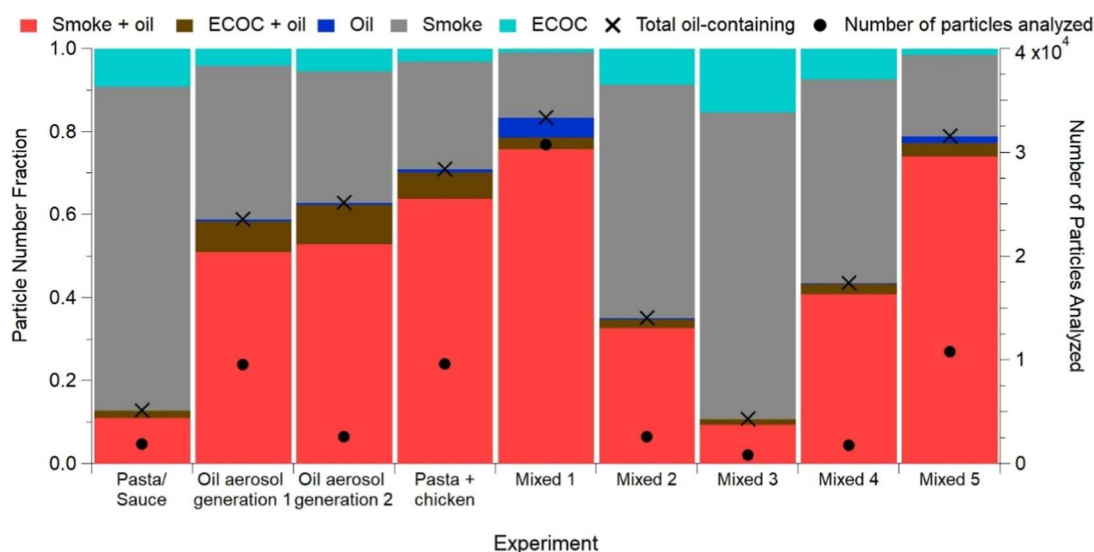


Figure 4. ATOFMS measured number fractions (0.07–2 μm) of each identified single-particle type and of all oil-containing particle types (left axis) during each cooking experiment, as described in Table 1. The total number of particles analyzed (right axis) during each experiment is also shown.

support that the background aerosol in the house largely corresponds to infiltration of outdoor aged aerosol.

Individual particles classified as smoke + oil produced mass spectral ion markers that were observed for both the smoke- and oil-dominant particle types (Figure 2), meaning chemical species from these two sources were mixed within individual particles. This smoke + oil single-particle mixture is likely the result of gas-particle partitioning of volatilized cooking oil onto pre-existing wood smoke particles, as well as coagulation with cooking oil particles. This shows that different emission sources (residential wood combustion and cooking oil) can be observed within the same individual particle, which is important as home heating and cooking often occur simultaneously. Even with no active pellet stove burning indoors (i.e., during nonmixed experiments), individual smoke + oil particles were observed during cooking experiments (discussed in Section 3.3) due to the presence of infiltrated residential heating emissions from outdoors. This finding further highlights the importance of understanding the mixing of residential home heating and cooking oil emissions as particles containing chemical species from both sources can coexist indoors, even without an indoor wood burning source present. The mixing of different chemical species from smoke and cooking indoors reported here may have implications for human health that are complex and require further investigation. It is well-established that inhalation of smoke can lead to various health issues,⁹⁸ and inhalation of cooking fumes has become of recent interest,³³ but inhalation of particles containing compounds from both smoke and cooking remains largely unconstrained.⁹⁹

The elemental carbon/organic carbon (ECOC) particle types were identified based on the presence of elemental carbon (e.g., C_n^+ , m/z 12, 24, 36,...) and organic carbon fragment (e.g., C_2H_3^+ , m/z 27) ions.^{100,101} Similar to the smoke particles discussed above, the ECOC particles were further classified as ECOC or ECOC + oil based on the presence of β/γ -tocopherol ($\text{C}_{28}\text{H}_{48}\text{O}_2^+$, m/z 416) and linolenate ($\text{C}_{18}\text{H}_{29}\text{O}_2^-$, m/z -277)^{63,65} (Figure 3). Both ECOC and ECOC + oil average single-particle mass spectra also show ions corresponding to nitrate (NO_2^- , m/z -46;

NO_3^- , m/z -62)¹⁰² and sulfate (HSO_4^- , m/z -97).⁸⁶ The ECOC + oil particle type mass spectra also show ion markers for the suite of fatty acids and mixed tocopherols observed in other cooking oil-containing particle types.

Similar to the background wood smoke particle type discussed above, the ECOC and ECOC + oil particle type mass spectra also show ion markers associated with secondary organic aerosol (oxygenated organic fragment: $\text{C}_2\text{H}_3\text{O}^+$, m/z 43)⁹⁵ and aqueous-phase reactions (oxalate: HC_2O_4^- , m/z -89).⁹⁶ The oxygenated organic fragment (m/z 43) was observed in $81.2 \pm 0.9\%$ and $73.4 \pm 0.8\%$ of the ECOC and ECOC + oil particles, respectively. Oxalate was observed in $15.9 \pm 0.8\%$ and $6.6 \pm 0.5\%$ of the ECOC and ECOC + oil particles, respectively. The presence of both of these marker ions indicates the individual ECOC and ECOC + oil particles had undergone accumulation of secondary organic aerosol, indicative of outdoor atmospheric aging reactions; however, the fraction of particles that contain these aging markers for these minor particle types is lower than for the indoor background smoke particles ($95.21 \pm 0.04\%$ for $\text{C}_2\text{H}_3\text{O}^+$ and $43.13 \pm 0.09\%$ for HC_2O_4^-). This suggests that the infiltrated ECOC particle types measured during the cooking experiments are less aged than the background smoke particles, potentially due to the ECOC particle types being less hygroscopic, taking up less water, and reducing aqueous-phase secondary organic aerosol formation.

It is important to note that for a particle to be chemically analyzed by the ATOFMS, it must absorb photons of the wavelength of the desorption/ionization laser (i.e., 266 nm). A previous ATOFMS study found that no positive or negative ions were observed for pure oleic acid particles due to its low molar absorptivity at 266 nm.⁹⁰ This is also supported by the low molar absorption coefficient ($\sim 1.1 \times 10^2 \text{ L mol}^{-1} \text{ cm}^{-1}$) of linoleic acid, one of the fatty acid markers in this study, at 266 nm.¹⁰³ As fatty acids are a major component of the oil-dominant particles, this suggests that the number fractions of the oil-dominant particles are expected to be lower limits due to this detection limitation. As a result, the fractional contributions from the other four individual particle types (i.e., smoke, smoke + cooking oil, ECOC, and ECOC +

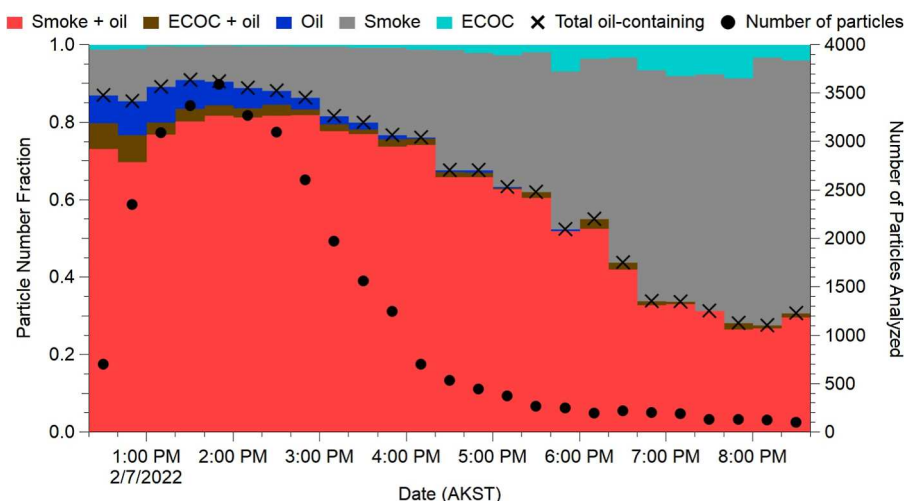


Figure 5. Number fractions of single-particle types, including the total number fraction of oil-containing particles (left), and total numbers of particles analyzed (right), per 20 min, after the mixed 1 experiment. Active cooking was from 12:22–12:40 AKST.

cooking oil) are likely upper limits due to the presence of other absorbing compounds (e.g., polycyclic aromatic hydrocarbons) that readily absorb 266 nm photons and produce single-particle mass spectra.¹⁰⁴

3.3. Smoke + Cooking Oil Particles Dominate Measured Number Fractions during Cooking Experiments. The smoke + cooking oil single-particle type accounted for 9–76%, by number, of the total individual particles (0.07–2 μm) measured by the ATOFMS during all cooking experiments, while the number fraction of the smoke single-particle type ranged from 16% to 78% (Figure 4). Generally, experiments were dominated either by particles classified as smoke or smoke + oil, showing the major contribution (90.7 \pm 0.1%, by number) from smoke (infiltrated wood smoke from outdoors and/or pellet stove emissions) to the indoor aerosol population during mixed experiments (Section 3.2). During experiments in which smoke + oil particles composed greater than 50% of the measured particle number fraction, the number fractions of the oil-dominant and ECOC + oil particle types were also higher. Specifically, other oil-containing particle types comprised 5–10% of the particle number fraction for experiments dominated by smoke + oil particles, compared to 1–3% for experiments with smoke + oil particle number fractions less than 50% (Figure 4). The large number fractions of the smoke + oil particles show that the cooking oil mixed with the pre-existing indoor smoke particles from the pellet stove and from infiltrated outdoor air. This is likely due to a combination of heated cooking oil volatilizing and condensing onto indoor smoke particles and the coagulation of ultrafine cooking-generated aerosol with pre-existing indoor smoke.

The mixed 1 and mixed 5 experiments (Table 1) had the highest number fractions of smoke + oil particles across the nine cooking experiments, with values of 75.9 \pm 0.2% and 74.0 \pm 0.4%, respectively. The high number fraction during the mixed 1 experiment was likely due to the high heat applied during cooking and subsequent chicken burning, which resulted in a large particle-phase fraction of cooking oil, as supported by the SV-TAG data (Figure S10). This is supported further by the mixed 1 experiment having the highest number fractions of oil-dominant and oil-containing (i.e., smoke + oil, oil-dominant, and ECOC + oil) particles at

4.7 \pm 0.1% and 83.3 \pm 0.1%, respectively (Figure 4). The generation of more cooking oil emissions during the mixed 1 experiment allowed for greater mixing with smoke produced from the pellet stove and resulted in the highest number fraction of smoke + oil particles. The highest number fraction of oil-containing particles (91.0 \pm 0.1%) during the mixed 1 experiment was observed 40 min after the active cooking period and decreased over time (Figure 5). The increasing number fraction of oil-containing particles aligns with the particle sizing data discussed in Section 3.1, which shows the highest aerosol growth rate for the first 30 min after active cooking during the mixed 1 experiment. We also examined the cooking oil ion abundances (proportional to mass) in the smoke + oil particle mass spectra for the mixed 1 experiment, with the highest ion signals for the fatty acids and tocopherols observed during and immediately after active cooking (Figure S11). This further supports the early roles of coagulation of cooking oil particles with the pre-existing pellet stove smoke particles as well as condensation of volatilized cooking oil onto the pre-existing pellet stove smoke particles. After the mixed 1 experiment activities, the contribution of smoke and ECOC particles (not containing cooking oil) to the measured particle number fraction increases (Figure 5) due to the removal of the pellet stove and cooking-generated aerosol through deposition, ventilation, and coagulation. This is expected as the indoor background aerosol is primarily composed of infiltrated wood smoke (Figure S6).

For two experiments, pasta/sauce and mixed 3, no oil-dominant particles were measured, and only small number fractions of oil-containing particles (12.8 \pm 0.1% and 10.8 \pm 0.1%, respectively) were measured. No cooking oil was used during the pasta/sauce experiment; however, soybean oil is a common ingredient in store-bought pasta sauce and therefore likely explains the small fraction of oil-containing particles observed. Despite the consistent cooking procedures implemented in this study (Section 2.1), variability in cooking occurred as the breaded chicken during the mixed 3 experiment was unintentionally cooked at a lower heat than in the other mixed experiments, resulting in the chicken not being fully cooked. This lower temperature resulted in a reduction in volatilized cooking oil and led to no oil-dominant particles being measured during this experiment. This is

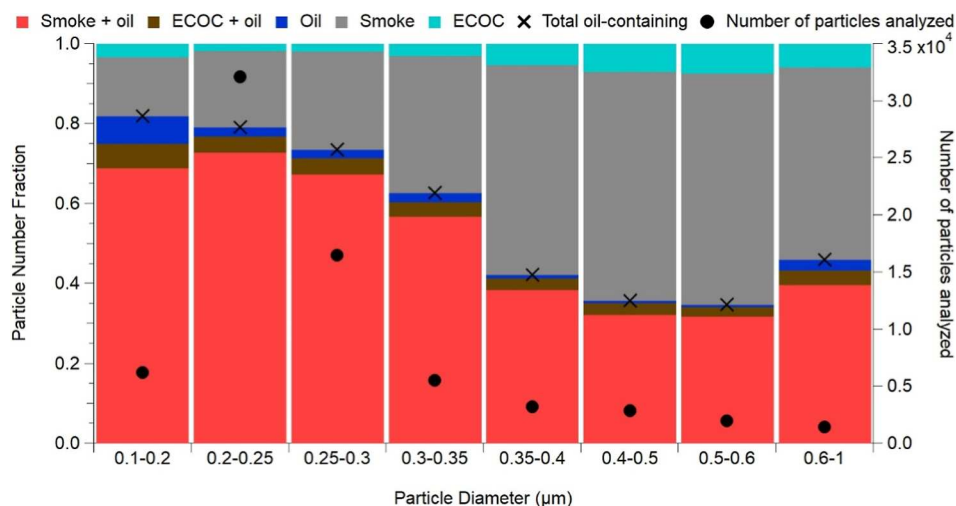


Figure 6. Size-resolved number fractions of single-particle types: smoke + oil, ECOC + oil, oil-dominant, smoke, and ECOC (left axis) and number of particles measured in each size bin range by the ATOFMS (right axis) during all nine cooking experiments.

supported by the low number of particles chemically analyzed by the ATOFMS for the mixed 3 experiment (Figure 4) and the lower particle number concentrations than in the other mixed experiments measured by the particle sizing instrumentation (Figure S3).

Of all the measured individual particle mass spectra that contained cooking oil marker ions, the largest number fraction of cooking oil-containing particles was from 0.1 to 0.2 μm d_{va} ($81.9 \pm 0.2\%$), and the number fraction decreased with increasing particle diameter, down to $45.9 \pm 0.3\%$ for 0.6–1 μm (largest size bin, as selected based on sufficient ATOFMS particle statistics; Figure 6). The increase in the number fraction of oil-containing particles from 0.6 to 1 μm compared to 0.5–0.6 μm could be a result of larger particles having more mass to uptake gaseous cooking emissions, thus increasing the number fraction of oil-containing particles at these larger particle diameters. Furthermore, we examined the cooking oil ion abundances in the smoke + oil particle mass spectra during the mixed 1 experiment as a function of the particle diameter. We found the highest ion abundance (proportional to mass) for all cooking oil species in the smallest size bin (0.1–0.2 μm), with decreasing abundance with increasing particle diameter (Figure S12). The greatest mass of cooking oil for smaller particle diameters agrees with smaller particles coagulating, as well as accumulating more semivolatile species via condensation based on the Kelvin effect. The number fraction of oil-dominant particles was also the largest from 0.1 to 0.2 μm (d_{va}) at $6.9 \pm 0.3\%$ and decreased with increasing particle diameter to a contribution of $0.5 \pm 0.1\%$, by number, from 0.4 to 0.5 μm (Figure 6). Based on prior literature^{41,105} and the cooking experiment particle size distribution data herein (Figures 1 and S1–S5), cooking-generated aerosol is typically dominated in number by ultrafine aerosol. This suggests that a large fraction of the ultrafine (<100 nm) particles below the ATOFMS measurement range likely contained cooking oil.

4. CONCLUSIONS

In this work, the chemical composition of individual indoor aerosol particles was measured during cooking experiments in a residential house in Fairbanks, AK, during the winter to broaden our understanding of chemistry in understudied

indoor environments. During cooking experiments, the majority of individual aerosol particles measured by the ATOFMS contained cooking oil components: fatty acids and mixed tocopherols. During periods without cooking, most of the measured particles were identified as smoke, from the indoor home heating pellet stove or from infiltration of outdoor residential heating emissions. During all nine cooking experiments, the majority of individual indoor particles, by number, existed as mixtures of cooking oil and smoke, resulting from the coagulation of pre-existing smoke particles with cooking oil particles and condensation of volatilized cooking soybean oil onto pre-existing smoke particles. This conclusion is supported by particle sizing data that showed that the average indoor particle mode diameter increased after all cooking periods.

The chemical composition of the indoor background aerosol in the house mainly consisted of smoke from the infiltration of outdoor residential home heating emissions. Residential wood combustion is a prominent aerosol source in high-latitude environments.⁵² Wood burning stoves have been shown to contribute to the indoor environment through direct emissions while burning¹⁰⁶ and from residential heating particles penetrating indoors from the outside, as observed in this study. Outside of wintertime environments, another important source of smoke includes wildfire emissions, which can also infiltrate indoors and impact indoor air quality.¹⁰⁷ Therefore, the results of mixed cooking oil and smoke particles are also relevant for this scenario, particularly given increasing wildfire smoke emissions across Alaska¹⁰⁸ and the Western U.S.¹⁰⁹ Furthermore, this study also shows that cooking oil can mix with other types of infiltrated combustion particles, including those generated from vehicle combustion.

Differences across indoor activities, especially cooking, can significantly impact the chemical and physical properties of the resulting emissions.⁴⁴ This variability is demonstrated in this study as replicates of cooking experiments yielded varying particle number concentrations, diameters, and individual chemical composition across experiments of the same type. In particular, replicate mixed (pellet stove + cooking) experiments were conducted and resulted in variations in the average particle number concentration by an order of magnitude, attributed to unintentional differences in cooking

temperature. Characterizing the indoor environment as realistically as possible, e.g., when multiple indoor sources are present simultaneously, is crucial to understand human exposure to particulate matter indoors. This work also shows that different indoor sources, such as a home heating pellet stove and cooking, can impact physical mixing of various gaseous and particulate emissions, which may result in unconstrained multiphase chemistry and uncertain health impacts. Therefore, it is essential to continue to study and understand the complex relationships that influence indoor air quality, particularly in understudied low-temperature environments, where other outdoor air infiltration sources and time spent indoors are expected to differ from those in warmer environments.

■ ASSOCIATED CONTENT

SI Supporting Information

The Supporting Information is available free of charge at <https://pubs.acs.org/doi/10.1021/acsestair.5c00156>.

SV-TAG methods and phase determination; discussion of coagulation calculations; coagulation calculation values; aerosol mode diameter and number concentration change vs time for additional cooking experiments; average ATOFMS mass spectra measured indoors during nonexperiment times; average ATOFMS mass spectra for additional cooking experiments; SV-TAG phase results; and fatty acid and tocopherol abundances versus time after cooking and versus particle diameter (PDF)

■ AUTHOR INFORMATION

Corresponding Author

Kerri A. Pratt – Department of Chemistry, University of Michigan, Ann Arbor, Michigan 48109, United States; Department of Earth and Environmental Sciences, University of Michigan, Ann Arbor, Michigan 48109, United States; orcid.org/0000-0003-4707-2290; Email: prattka@umich.edu

Authors

Logan Forshee – Department of Chemistry, University of Michigan, Ann Arbor, Michigan 48109, United States; orcid.org/0009-0009-3492-7764
Andrew L. Holen – Department of Chemistry, University of Michigan, Ann Arbor, Michigan 48109, United States; orcid.org/0009-0006-7654-2019
Judy Wu – Department of Chemistry, University of Michigan, Ann Arbor, Michigan 48109, United States; orcid.org/0000-0003-3541-4492
Karolina Cysneiros de Carvalho – Department of Energy, Environmental and Chemical Engineering, Washington University in St. Louis, St. Louis, Missouri 63130, United States; Present Address: Department of Environmental Sciences, University of California, Riverside, Riverside, CA, United States
Vanessa Selimovic – Department of Chemistry, University of Michigan, Ann Arbor, Michigan 48109, United States; Department of Chemistry and Biochemistry, University of Montana, Missoula, Montana 59812, United States; orcid.org/0000-0002-3053-2732
Ellis S. Robinson – Department of Environmental Health and Engineering, Johns Hopkins University, Baltimore, Maryland

21218, United States; Present Address: Department of Chemical and Environmental Engineering, University of Arizona, Tucson, AZ, United States; orcid.org/0000-0003-1695-6392

Damien T. Ketcherside – Department of Chemistry and Biochemistry, University of Montana, Missoula, Montana 59812, United States; orcid.org/0000-0002-2149-9133

Sukriti Kapur – Department of Chemistry, University of California Irvine, Irvine, California 92697, United States; orcid.org/0000-0001-6645-7300

Andrew P. Ault – Department of Chemistry, University of Michigan, Ann Arbor, Michigan 48109, United States; orcid.org/0000-0002-7313-8559

Lu Hu – Department of Chemistry and Biochemistry, University of Montana, Missoula, Montana 59812, United States

Brent J. Williams – Department of Energy, Environmental and Chemical Engineering, Washington University in St. Louis, St. Louis, Missouri 63130, United States; Present Address: Department of Soil, Water, and Climate, University of Minnesota, St. Paul, MN, United States

Peter F. DeCarlo – Department of Environmental Health and Engineering, Johns Hopkins University, Baltimore, Maryland 21218, United States; orcid.org/0000-0001-6385-7149

Complete contact information is available at:

<https://pubs.acs.org/doi/10.1021/acsestair.5c00156>

Notes

The authors declare no competing financial interest.

■ ACKNOWLEDGMENTS

The ALPACA project was initiated as a part of the Air Pollution in the Arctic: Climate, Environment and Societies (PACES) activity under the International Global Atmospheric Chemistry (IGAC) Project. We thank William R. Simpson, the University of Alaska-Fairbanks, and the ALPACA research team for logistical fieldwork assistance and collaborations. L.F., A.L.H., J.W., V.S., and K.A.P. acknowledge support from the National Science Foundation (NSF) grant NNA-1927831. The University of Michigan also provided supplemental support during this research. K.C.d.C. and B.J.W. acknowledge support from the NSF grant NNA-1927867. D.T.K., V.S., and L.H. were supported by the NOAA Climate Program Office's Atmospheric Chemistry, Carbon Cycle, and Climate program, grant number NA20OAR4310296. S.K. acknowledges funding from the U.S. National Science Foundation (AGS-1654104, CHE-2203419). E.S.R. and P.F.D. acknowledge funding support from the NSF grant NNA-2012905.

■ REFERENCES

- (1) Klepeis, N.; Nelson, W.; Ott, W.; Robinson, J.; Tsang, A.; Switzer, P.; Behar, J.; Hern, S.; Engelmann, W. The National Human Activity Pattern Survey (NHAPS): A Resource for Assessing Exposure to Environmental Pollutants. *J. Expo. Anal. Environ. Epidemiol.* **2001**, *11*, 231–252.
- (2) Fares, A. Seasonality of Tuberculosis. *J. Glob. Infect. Dis.* **2011**, *3* (1), 46–55.
- (3) González-Martín, J.; Kraakman, N. J. R.; Pérez, C.; Lebrero, R.; Muñoz, R. A State-of-the-Art Review on Indoor Air Pollution and Strategies for Indoor Air Pollution Control. *Chemosphere* **2021**, *262*, 128376.
- (4) Avery, A. M.; Waring, M. S.; DeCarlo, P. F. Seasonal Variation in Aerosol Composition and Concentration upon Transport from the

- Outdoor to Indoor Environment. *Environ. Sci.:Processes Impacts* **2019**, *21* (3), 528–547.
- (5) Fu, N.; Kim, M. K.; Chen, B.; Sharples, S. Investigation of Outdoor Air Pollutant, PM_{2.5} Affecting the Indoor Air Quality in a High-Rise Building. *Indoor Built Environ.* **2022**, *31* (4), 895–912.
- (6) Fu, N.; Kim, M. K.; Huang, L.; Liu, J.; Chen, B.; Sharples, S. Experimental and Numerical Analysis of Indoor Air Quality Affected by Outdoor Air Particulate Levels (PM_{1.0}, PM_{2.5} and PM₁₀), Room Infiltration Rate, and Occupants' Behaviour. *Sci. Total Environ.* **2022**, *851*, 158026.
- (7) Johnson, A. M.; Waring, M. S.; DeCarlo, P. F. Real-Time Transformation of Outdoor Aerosol Components upon Transport Indoors Measured with Aerosol Mass Spectrometry. *Indoor Air* **2017**, *27* (1), 230–240.
- (8) Rackes, A.; Waring, M. S. Modeling Impacts of Dynamic Ventilation Strategies on Indoor Air Quality of Offices in Six US Cities. *Builde. Environ.* **2013**, *60*, 243–253.
- (9) Patel, S.; Sankhyan, S.; Boedicker, E. K.; DeCarlo, P. F.; Farmer, D. K.; Goldstein, A. H.; Katz, E. F.; Nazaroff, W. W.; Tian, Y.; Vanhanen, J.; Vance, M. E. Indoor Particulate Matter during HOMEChem: Concentrations, Size Distributions, and Exposures. *Environ. Sci. Technol.* **2020**, *54* (12), 7107–7116.
- (10) Wallace, L. Indoor Sources of Ultrafine and Accumulation Mode Particles: Size Distributions, Size-Resolved Concentrations, and Source Strengths. *Aerosol Sci. Technol.* **2006**, *40* (5), 348–360.
- (11) Nazaroff, W. W.; Weschler, C. J. Cleaning Products and Air Fresheners: Exposure to Primary and Secondary Air Pollutants. *Atmos. Environ.* **2004**, *38* (18), 2841–2865.
- (12) Singer, B. C.; Coleman, B. K.; Destailats, H.; Hodgson, A. T.; Lunden, M. M.; Weschler, C. J.; Nazaroff, W. W. Indoor Secondary Pollutants from Cleaning Product and Air Freshener Use in the Presence of Ozone. *Atmos. Environ.* **2006**, *40* (35), 6696–6710.
- (13) Brauer, M.; Hirtle, R.; Lang, B.; Ott, W. Assessment of Indoor Fine Aerosol Contributions from Environmental Tobacco Smoke and Cooking with a Portable Nephelometer. *J. Expo. Sci. Environ. Epidemiol.* **2000**, *10* (2), 136–144.
- (14) DeCarlo, P. F.; Avery, A. M.; Waring, M. S. Thirdhand Smoke Uptake to Aerosol Particles in the Indoor Environment. *Sci. Adv.* **2018**, *4* (5), No. eaap8368.
- (15) Repace, J. L.; Lowrey, A. H. Indoor Air Pollution, Tobacco Smoke, and Public Health. *Science* **1980**, *208* (4443), 464–472.
- (16) Rádis-Baptista, G. Do Synthetic Fragrances in Personal Care and Household Products Impact Indoor Air Quality and Pose Health Risks? *J. Xenobiotics* **2023**, *13* (1), 121–131.
- (17) Uhde, E.; Salthammer, T. Impact of Reaction Products from Building Materials and Furnishings on Indoor Air Quality—A Review of Recent Advances in Indoor Chemistry. *Atmos. Environ.* **2007**, *41* (15), 3111–3128.
- (18) Avery, A. M.; Waring, M. S.; DeCarlo, P. F. Human Occupant Contribution to Secondary Aerosol Mass in the Indoor Environment. *Environ. Sci.:Processes Impacts* **2019**, *21* (8), 1301–1312.
- (19) Nazaroff, W. W.; Goldstein, A. H. Indoor Chemistry: Research Opportunities and Challenges. *Indoor Air* **2015**, *25* (4), 357–361.
- (20) Fortenberry, C.; Walker, M.; Dang, A.; Loka, A.; Date, G.; Cysneiros de Carvalho, K.; Morrison, G.; Williams, B. Analysis of Indoor Particles and Gases and Their Evolution with Natural Ventilation. *Indoor Air* **2019**, *29* (5), 761–779.
- (21) O'Brien, R. E.; Li, Y.; Kiland, K. J.; Katz, E. F.; Or, V. W.; Legaard, E.; Walkout, E. Q.; Thrasher, C.; Grassian, V. H.; DeCarlo, P. F.; Bertram, A. K.; Shiraiwa, M. Emerging Investigator Series: Chemical and Physical Properties of Organic Mixtures on Indoor Surfaces during HOMEChem. *Environ. Sci.:Processes Impacts* **2021**, *23* (4), 559–568.
- (22) Abbatt, D.; Wang, C. The Atmospheric Chemistry of Indoor Environments. *Environ. Sci.:Processes Impacts* **2020**, *22* (1), 25–48.
- (23) Tham, K. W. Indoor Air Quality and Its Effects on Humans—A Review of Challenges and Developments in the Last 30 Years. *Energy Build.* **2016**, *130*, 637–650.
- (24) Spengler, J. D.; Dockery, D. W.; Turner, W. A.; Wolfson, J. M.; Ferris, B. G. Long-Term Measurements of Respirable Sulfates and Particles inside and Outside Homes. *Atmos. Environ.* **1981**, *15* (1), 23–30.
- (25) Tofful, L.; Canepari, S.; Sargolini, T.; Perrino, C. Indoor Air Quality in a Domestic Environment: Combined Contribution of Indoor and Outdoor PM Sources. *Builde. Environ.* **2021**, *202*, 108050.
- (26) Tu, K.-W.; Knutson, E. O. Indoor Outdoor Aerosol Measurements for Two Residential Buildings in New Jersey. *Aerosol Sci. Technol.* **1988**, *9* (1), 71–82.
- (27) Pope, C. A.; Dockery, D. W.; Spengler, J. D.; Raizenne, M. E. Respiratory Health and PM₁₀ Pollution. A Daily Time Series Analysis. *Am. Rev. Respir. Dis.* **1991**, *144* (3 pt 1), 668–674.
- (28) Cohen, A. J.; Brauer, M.; Burnett, R.; Anderson, H. R.; Frostad, J.; Estep, K.; Balakrishnan, K.; Brunekreef, B.; Dandona, L.; Dandona, R.; Feigin, V.; Freedman, G.; Hubbell, B.; Jobling, A.; Kan, H.; Knibbs, L.; Liu, Y.; Martin, R.; Morawska, L.; Pope, C. A.; Shin, H.; Straif, K.; Shaddick, G.; Thomas, M.; van Dingenen, R.; van Donkelaar, A.; Vos, T.; Murray, C. J. L.; Forouzanfar, M. H. Estimates and 25-Year Trends of the Global Burden of Disease Attributable to Ambient Air Pollution: An Analysis of Data from the Global Burden of Diseases Study 2015. *Lancet* **2017**, *389* (10082), 1907–1918.
- (29) Shi, L.; Zhu, Q.; Wang, Y.; Hao, H.; Zhang, H.; Schwartz, J.; Amini, H.; van Donkelaar, A.; Martin, R. V.; Steenland, K.; Sarnat, J. A.; Caudle, W. M.; Ma, T.; Li, H.; Chang, H. H.; Liu, J. Z.; Wingo, T.; Mao, X.; Russell, A. G.; Weber, R. J.; Liu, P. Incident Dementia and Long-Term Exposure to Constituents of Fine Particle Air Pollution: A National Cohort Study in the United States. *Proc. Natl. Acad. Sci. U.S.A.* **2023**, *120* (1), No. e2211282119.
- (30) Pope, C. A.; Dockery, D. W. Health Effects of Fine Particulate Air Pollution: Lines That Connect. *J. Air Waste Manag. Assoc.* **2006**, *56* (6), 709–742.
- (31) Alves, C. A.; Vicente, E. D.; Evtugina, M.; Vicente, A. M. P.; Sainnokhoi, T.-A.; Kováts, N. Cooking Activities in a Domestic Kitchen: Chemical and Toxicological Profiling of Emissions. *Sci. Total Environ.* **2021**, *772*, 145412.
- (32) Du, B.; Gao, J.; Chen, J.; Stevanovic, S.; Ristovski, Z.; Wang, L.; Wang, L. Particle Exposure Level and Potential Health Risks of Domestic Chinese Cooking. *Builde. Environ.* **2017**, *123*, 564–574.
- (33) Ding, R.; Zhang, C.; Zhu, X.; Cheng, H.; Zhu, F.; Xu, Y.; Liu, Y.; Wen, L.; Cao, J. ROS-AKT-mTOR Axis Mediates Autophagy of Human Umbilical Vein Endothelial Cells Induced by Cooking Oil Fumes-Derived Fine Particulate Matters in Vitro. *Free Radic. Biol. Med.* **2017**, *113*, 452–460.
- (34) Kapur, S.; Edwards, K. C.; Fang, T.; Schervish, M.; Lakey, P. S. J.; Yang, Y.; Robinson, E. S.; DeCarlo, P. F.; Simpson, W. R.; Weber, R. J.; Shiraiwa, M. Reactive Oxygen Species, Environmentally Persistent Free Radicals, and Oxidative Potential of Outdoor and Indoor Particulate Matter in Wintertime Fairbanks, Alaska. *Aerosol Sci. Technol.* **2024**, *59* (10), 1180–1197.
- (35) Yang, Y.; Battaglia, M. A.; Robinson, E. S.; DeCarlo, P. F.; Edwards, K. C.; Fang, T.; Kapur, S.; Shiraiwa, M.; Cesler-Maloney, M.; Simpson, W. R.; Campbell, J. R.; Nenes, A.; Mao, J.; Weber, R. J. Indoor–Outdoor Oxidative Potential of PM_{2.5} in Wintertime Fairbanks, Alaska: Impact of Air Infiltration and Indoor Activities. *ACS EST Air* **2024**, *1* (3), 188–199.
- (36) Schraufnagel, D. E. The Health Effects of Ultrafine Particles. *Exp. Mol. Med.* **2020**, *52* (3), 311–317.
- (37) Bi, J.; Lin, Z.; Li, Y.; Chen, F.; Liu, S.; Li, C. Effects of Different Cooking Methods on Volatile Flavor Compounds of Chicken Breast. *J. Food Biochem.* **2021**, *45* (8), No. e13770.
- (38) Masoud, C. G.; Li, Y.; Wang, D. S.; Katz, E. F.; DeCarlo, P. F.; Farmer, D. K.; Vance, M. E.; Shiraiwa, M.; Hildebrandt Ruiz, L. Molecular Composition and Gas-Particle Partitioning of Indoor Cooking Aerosol: Insights from a FIGAERO-CIMS and Kinetic Aerosol Modeling. *Aerosol Sci. Technol.* **2022**, *56* (12), 1156–1173.
- (39) Zeng, J.; Yu, Z.; Mekic, M.; Liu, J.; Li, S.; Loisel, G.; Gao, W.; Gandolfo, A.; Zhou, Z.; Wang, X.; Herrmann, H.; Gligorovski, S.; Li,

- X. Evolution of Indoor Cooking Emissions Captured by Using Secondary Electrospray Ionization High-Resolution Mass Spectrometry. *Environ. Sci. Technol. Lett.* **2020**, *7* (2), 76–81.
- (40) Kamens, R.; Lee, C.; Wiener, R.; Leith, D. A Study of Characterize Indoor Particles in Three Non-Smoking Homes. *Atmos. Environ., Part A* **1991**, *25* (5), 939–948.
- (41) Wan, M.-P.; Wu, C.-L.; Sze To, G.-N.; Chan, T.-C.; Chao, C. Y. H. Ultrafine Particles, and PM_{2.5} Generated from Cooking in Homes. *Atmos. Environ.* **2011**, *45* (34), 6141–6148.
- (42) Buonanno, G.; Morawska, L.; Stabile, L. Particle Emission Factors during Cooking Activities. *Atmos. Environ.* **2009**, *43* (20), 3235–3242.
- (43) Alves, C. A.; Vicente, E. D.; Evtuygina, M.; Vicente, A. M. P.; Sainnokhoi, T.-A.; Kováts, N. Cooking Activities in a Domestic Kitchen: Chemical and Toxicological Profiling of Emissions. *Sci. Total Environ.* **2021**, *772*, 145412.
- (44) Abdullahi, K. L.; Delgado-Saborit, J. M.; Harrison, R. M. Emissions and Indoor Concentrations of Particulate Matter and Its Specific Chemical Components from Cooking: A Review. *Atmos. Environ.* **2013**, *71*, 260–294.
- (45) Brown, W. L.; Day, D. A.; Stark, H.; Pagonis, D.; Krechmer, J. E.; Liu, X.; Price, D. J.; Katz, E. F.; DeCarlo, P. F.; Masoud, C. G.; Wang, D. S.; Hildebrandt Ruiz, L.; Arata, C.; Lunderberg, D. M.; Goldstein, A. H.; Farmer, D. K.; Vance, M. E.; Jimenez, J. L. Real-Time Organic Aerosol Chemical Speciation in the Indoor Environment Using Extractive Electrospray Ionization Mass Spectrometry. *Indoor Air* **2021**, *31* (1), 141–155.
- (46) Pothier, M. A.; Boedicker, E.; Pierce, J. R.; Vance, M.; Farmer, D. K. From the HOMEChem Frying Pan to the Outdoor Atmosphere: Chemical Composition, Volatility Distributions and Fate of Cooking Aerosol. *Environ. Sci.:Processes Impacts* **2023**, *25* (2), 314–325.
- (47) Lunderberg, D. M.; Kristensen, K.; Tian, Y.; Arata, C.; Misztal, P. K.; Liu, Y.; Kreisberg, N.; Katz, E. F.; DeCarlo, P. F.; Patel, S.; Vance, M. E.; Nazaroff, W. W.; Goldstein, A. H. Surface Emissions Modulate Indoor SVOC Concentrations through Volatility-Dependent Partitioning. *Environ. Sci. Technol.* **2020**, *54* (11), 6751–6760.
- (48) Ma, T.; Furutani, H.; Duan, F.; Ma, Y.; Toyoda, M.; Kimoto, T.; Huang, T.; He, K. Real-Time Single-Particle Characteristics and Aging of Cooking Aerosols in Urban Beijing. *Environ. Sci. Technol. Lett.* **2023**, *10*, 404.
- (49) Dall'Osto, M.; Harrison, R. M.; Charpantidou, E.; Loupa, G.; Rapsomanikis, S. Characterisation of Indoor Airborne Particles by Using Real-Time Aerosol Mass Spectrometry. *Sci. Total Environ.* **2007**, *384* (1), 120–133.
- (50) Schmale, J.; Arnold, S. R.; Law, K. S.; Thorp, T.; Anenberg, S.; Simpson, W. R.; Mao, J.; Pratt, K. A. Local Arctic Air Pollution: A Neglected but Serious Problem. *Earths Future* **2018**, *6* (10), 1385–1412.
- (51) Busby, B. D.; Ward, T. J.; Turner, J. R.; Palmer, C. P. Comparison and Evaluation of Methods to Apportion Ambient PM_{2.5} to Residential Wood Heating in Fairbanks, AK. *Aerosol Air Qual. Res.* **2016**, *16* (3), 492–503.
- (52) Wang, Y.; Hopke, P. K. Is Alaska Truly the Great Escape from Air Pollution? - Long Term Source Apportionment of Fine Particulate Matter in Fairbanks, Alaska. *Aerosol Air Qual. Res.* **2014**, *14* (7), 1875–1882.
- (53) Ward, T.; Trost, B.; Conner, J.; Flanagan, J.; Jayanty, R. K. M. Source Apportionment of PM_{2.5} in a Subarctic Airshed - Fairbanks, Alaska. *Aerosol Air Qual. Res.* **2012**, *12* (4), 536–543.
- (54) Simpson, W. R.; Mao, J.; Fochesatto, G. J.; Law, K. S.; DeCarlo, P. F.; Schmale, J.; Pratt, K. A.; Arnold, S. R.; Stutz, J.; Dibb, J. E.; Creamean, J. M.; Weber, R. J.; Williams, B. J.; Alexander, B.; Hu, L.; Yokelson, R. J.; Shiraiwa, M.; Decesari, S.; Anastasio, C.; D'Anna, B.; Gilliam, R. C.; Nenes, A.; St Clair, J. M.; Trost, B.; Flynn, J. H.; Savarino, J.; Conner, L. D.; Kettle, N.; Heeringa, K. M.; Albertin, S.; Baccarini, A.; Barret, B.; Battaglia, M. A.; Bekki, S.; Brado, T. J.; Brett, N.; Brus, D.; Campbell, J. R.; Cesler-Maloney, M.; Cooperdock, S.; Cysneiros de Carvalho, K.; Delbarre, H.; DeMott, P. J.; Dennehy, C. J.; Dieudonné, E.; Dingilian, K. K.; Donato, A.; Douglis, K. M.; Edwards, K. C.; Fahey, K.; Fang, T.; Guo, F.; Heinlein, L. M. D.; Hohen, A. L.; Huff, D.; Ijaz, A.; Johnson, S.; Kapur, S.; Ketcherside, D. T.; Levin, E.; Lill, E.; Moon, A. R.; Onishi, T.; Pappaccogli, G.; Perkins, R.; Pohorsky, R.; Raut, J.-C.; Ravetta, F.; Roberts, T.; Robinson, E. S.; Scoto, F.; Selimovic, V.; Sunday, M. O.; Temime-Roussel, B.; Tian, X.; Wu, J.; Yang, Y. Overview of the Alaskan Layered Pollution and Chemical Analysis (ALPACA) Field Experiment. *ACS EST Air* **2024**, *1* (3), 200–222.
- (55) Gunch, M. J.; Kirpes, R. M.; Kolesar, K. R.; Barrett, T. E.; China, S.; Sheesley, R. J.; Laskin, A.; Wiedensohler, A.; Tuch, T.; Pratt, K. A. Contributions of Transported Prudhoe Bay Oil Field Emissions to the Aerosol Population in Utqiagvik, Alaska. *Atmospheric Chem. Phys.* **2017**, *17* (17), 10879–10892.
- (56) Pratt, K. A.; Mayer, J. E.; Holecek, J. C.; Moffet, R. C.; Sanchez, R. O.; Rebotier, T. P.; Furutani, H.; Gonin, M.; Fuhrer, K.; Su, Y.; Guazzotti, S.; Prather, K. A. Development and Characterization of an Aircraft Aerosol Time-of-Flight Mass Spectrometer. *Anal. Chem.* **2009**, *81* (5), 1792–1800.
- (57) Williams, B. J.; Goldstein, A. H.; Kreisberg, N. M.; Hering, S. V. An In-Situ Instrument for Speciated Organic Composition of Atmospheric Aerosols: Thermal Desorption Aerosol GC/MS-FID (TAG). *Aerosol Sci. Technol.* **2006**, *40* (8), 627–638.
- (58) Zhao, Y.; Kreisberg, N. M.; Worton, D. R.; Teng, A. P.; Hering, S. V.; Goldstein, A. H. Development of an In Situ Thermal Desorption Gas Chromatography Instrument for Quantifying Atmospheric Semi-Volatile Organic Compounds. *Aerosol Sci. Technol.* **2013**, *47* (3), 258–266.
- (59) Khlystov, A.; Stanier, C.; Pandis, S. N. An Algorithm for Combining Electrical Mobility and Aerodynamic Size Distributions Data When Measuring Ambient Aerosol Special Issue of Aerosol Science and Technology on Findings from the Fine Particulate Matter Supersites Program. *Aerosol Sci. Technol.* **2004**, *38* (sup1), 229–238.
- (60) Moffet, R. C.; Qin, X.; Rebotier, T.; Furutani, H.; Prather, K. A. Chemically Segregated Optical and Microphysical Properties of Ambient Aerosols Measured in a Single-Particle Mass Spectrometer. *J. Geophys. Res.:Atmos.* **2008**, *113* (D12), 9393.
- (61) Zelenyuk, A.; Imre, D.; Han, J.-H.; Oatis, S. Simultaneous Measurements of Individual Ambient Particle Size, Composition, Effective Density, and Hygroscopicity. *Anal. Chem.* **2008**, *80* (5), 1401–1407.
- (62) Sultana, C. M.; Cornwell, G. C.; Rodriguez, P.; Prather, K. A. FATES: A Flexible Analysis Toolkit for the Exploration of Single-Particle Mass Spectrometer Data. *Atmospheric Meas. Technol.* **2017**, *10* (4), 1323–1334.
- (63) Jiang, K.; Gachumi, G.; Poudel, A.; Shurmer, B.; Bashi, Z.; El-Anead, A. The Establishment of Tandem Mass Spectrometric Fingerprints of Phytosterols and Tocopherols and the Development of Targeted Profiling Strategies in Vegetable Oils. *J. Am. Soc. Mass Spectrom.* **2019**, *30* (9), 1700–1712.
- (64) Inoue, T.; Tatemori, S.; Muranaka, N.; Hirahara, Y.; Homma, S.; Nakane, T.; Takano, A.; Nomi, Y.; Otsuka, Y. The Identification of Vitamin E Homologues in Medicinal Plant Samples Using ESI(+)-LC-MS3. *J. Agric. Food Chem.* **2012**, *60* (38), 9581–9588.
- (65) Catharino, R. R.; Haddad, R.; Cabrini, L. G.; Cunha, I. B. S.; Sawaya, A. C. H. F.; Eberlin, M. N. Characterization of Vegetable Oils by Electrospray Ionization Mass Spectrometry Fingerprinting: Classification, Quality, Adulteration, and Aging. *Anal. Chem.* **2005**, *77* (22), 7429–7433.
- (66) Lee, J. Y.; Daube, C.; Fortner, E.; Ellsworth, N.; May, N. W.; Tallant, J.; Herndon, S.; Pratt, K. A. Chemical Characterization of Prescribed Burn Emissions from a Mixed Forest in Northern Michigan. *Environ. Sci.: Atmos.* **2023**, *3* (1), 35–48.
- (67) Pratt, K. A.; Murphy, S. M.; Subramanian, R.; DeMott, P. J.; Kok, G. L.; Campos, T.; Rogers, D. C.; Prenni, A. J.; Heymsfield, A. J.; Seinfeld, J. H.; Prather, K. A. Flight-Based Chemical Characterization of Biomass Burning Aerosols within Two Prescribed Burn Smoke Plumes. *Atmospheric Chem. Phys.* **2011**, *11* (24), 12549–12565.

- (68) Hudson, P. K.; Murphy, D. M.; Cziczo, D. J.; Thomson, D. S.; de Gouw, J. A.; Warneke, C.; Holloway, J.; Jost, H.-J.; Hübler, G. Biomass-Burning Particle Measurements: Characteristic Composition and Chemical Processing. *J. Geophys. Res.:Atmos.* **2004**, *109* (D23), 4398.
- (69) Toner, S. M.; Shields, L. G.; Sodeman, D. A.; Prather, K. A. Using Mass Spectral Source Signatures to Apportion Exhaust Particles from Gasoline and Diesel Powered Vehicles in a Freeway Study Using UF-ATOFMS. *Atmos. Environ.* **2008**, *42* (3), 568–581.
- (70) Sodeman, D. A.; Toner, S. M.; Prather, K. A. Determination of Single Particle Mass Spectral Signatures from Light-Duty Vehicle Emissions. *Environ. Sci. Technol.* **2005**, *39* (12), 4569–4580.
- (71) Morawska, L.; He, C.; Hitchins, J.; Gilbert, D.; Parappukkaran, S. The Relationship between Indoor and Outdoor Airborne Particles in the Residential Environment. *Atmos. Environ.* **2001**, *35* (20), 3463–3473.
- (72) Bari, M. A.; Baumbach, G.; Brodbeck, J.; Struschka, M.; Kuch, B.; Dreher, W.; Scheffknecht, G. Characterisation of Particulates and Carcinogenic Polycyclic Aromatic Hydrocarbons in Wintertime Wood-Fired Heating in Residential Areas. *Atmos. Environ.* **2011**, *45* (40), 7627–7634.
- (73) Sankhyan, S.; Zabinski, K.; O'Brien, R. E.; Coyan, S.; Patel, S.; Vance, E.; Aerosol, M. Aerosol emissions and their volatility from heating different cooking oils at multiple temperatures. *Environ. Sci.: Atmos.* **2022**, *2* (6), 1364–1375.
- (74) Glytsos, T.; Ondráček, J.; Džumbová, L.; Kopanakis, I.; Lazaridis, M. Characterization of Particulate Matter Concentrations during Controlled Indoor Activities. *Atmos. Environ.* **2010**, *44* (12), 1539–1549.
- (75) Nazaroff, W. W. Indoor Particle Dynamics. *Indoor Air* **2004**, *14* (s7), 175–183.
- (76) Stephens, B.; Siegel, J. A. Ultrafine Particle Removal by Residential Heating, Ventilating, and Air-Conditioning Filters. *Indoor Air* **2013**, *23* (6), 488–497.
- (77) Xiao, Y.; Lv, Y.; Zhou, Y.; Liu, H.; Liu, J. Size-Resolved Surface Deposition and Coagulation of Indoor Particles. *Int. J. Environ. Health Res.* **2020**, *30* (3), 251–267.
- (78) Anand, S.; Sreekanth, B.; Mayya, Y. S. Effective Coagulation Coefficient Approach for Estimating Particle Number Emission Rates for Strong Emission Sources. *Aerosol Air Qual. Res.* **2016**, *16* (7), 1541–1547.
- (79) Carpenter, D. L.; Lehmann, J.; Mason, B. S.; Slover, H. T. Lipid Composition of Selected Vegetable Oils. *J. Am. Oil Chem. Soc.* **1976**, *53* (12), 713–718.
- (80) Passig, J.; Schade, J.; Irsig, R.; Kröger-Badge, T.; Czech, H.; Adam, T.; Fallgren, H.; Moldanova, J.; Sklorz, M.; Streibel, T.; Zimmermann, R. Single-Particle Characterization of Polycyclic Aromatic Hydrocarbons in Background Air in Northern Europe. *Atmospheric Chem. Phys.* **2022**, *22* (2), 1495–1514.
- (81) Rogge, W. F.; Hildemann, L. M.; Mazurek, M. A.; Cass, G. R.; Simoneit, B. R. T. Sources of Fine Organic Aerosol. 9. Pine, Oak, and Synthetic Log Combustion in Residential Fireplaces. *Environ. Sci. Technol.* **1998**, *32* (1), 13–22.
- (82) Linoleic acid (CAS RN: 60-33-3). <https://haz-map.com/Agents/5844> (accessed Sep 23, 2025).
- (83) alpha-Tocopherol (CAS RN: 59-02-9), Haz-Map. <https://haz-map.com/Agents/18658> (accessed Sep 23, 2025).
- (84) Pankow, J. F. An Absorption Model of the Gas/Aerosol Partitioning Involved in the Formation of Secondary Organic Aerosol. *Atmos. Environ.* **1994**, *28* (2), 189–193.
- (85) Williams, B. J.; Goldstein, A. H.; Kreisberg, N. M.; Hering, S. V. In Situ Measurements of Gas/Particle-Phase Transitions for Atmospheric Semivolatile Organic Compounds. *Proc. Natl. Acad. Sci. U.S.A.* **2010**, *107* (15), 6676–6681.
- (86) Neubauer, K. R.; Sum, S. T.; Johnston, M. V.; Wexler, A. S. Sulfur Speciation in Individual Aerosol Particles. *J. Geophys. Res.:Atmos.* **1996**, *101* (D13), 18701–18707.
- (87) Fine, P. M.; Cass, G. R.; Simoneit, B. R. T. Chemical Characterization of Fine Particle Emissions from Fireplace Combustion of Woods Grown in the Northeastern United States. *Environ. Sci. Technol.* **2001**, *35* (13), 2665–2675.
- (88) Heringa, M. F.; DeCarlo, P. F.; Chirico, R.; Lauber, A.; Doberer, A.; Good, J.; Nussbaumer, T.; Keller, A.; Burtscher, H.; Richard, A.; Miljevic, B.; Prevot, A. S. H.; Baltensperger, U. Time-Resolved Characterization of Primary Emissions from Residential Wood Combustion Appliances. *Environ. Sci. Technol.* **2012**, *46* (20), 11418–11425.
- (89) Qin, X.; Prather, K. A. Impact of Biomass Emissions on Particle Chemistry during the California Regional Particulate Air Quality Study. *Int. J. Mass Spectrom.* **2006**, *258* (1), 142–150.
- (90) Silva, P. J.; Prather, K. A. Interpretation of Mass Spectra from Organic Compounds in Aerosol Time-of-Flight Mass Spectrometry. *Anal. Chem.* **2000**, *72* (15), 3553–3562.
- (91) Simoneit, B. R. T.; Schauer, J. J.; Nolte, C. G.; Oros, D. R.; Elias, V. O.; Fraser, M. P.; Rogge, W. F.; Cass, G. R. Levoglucosan, a Tracer for Cellulose in Biomass Burning and Atmospheric Particles. *Atmos. Environ.* **1999**, *33* (2), 173–182.
- (92) Fortenberry, C. F.; Walker, M. J.; Zhang, Y.; Mitroo, D.; Brune, W. H.; Williams, B. J. Bulk and Molecular-Level Characterization of Laboratory-Aged Biomass Burning Organic Aerosol from Oak Leaf and Heartwood Fuels. *Atmospheric Chem. Phys.* **2018**, *18* (3), 2199–2224.
- (93) Hennigan, C. J.; Sullivan, A. P.; Collett, J. L.; Robinson, A. L. Levoglucosan Stability in Biomass Burning Particles Exposed to Hydroxyl Radicals. *Geophys. Res. Lett.* **2010**, *37* (9), 43088.
- (94) Schmidl, C.; Bauer, H.; Dattler, A.; Hitznerberger, R.; Weissenboeck, G.; Marr, I. L.; Puxbaum, H. Chemical Characterisation of Particle Emissions from Burning Leaves. *Atmos. Environ.* **2008**, *42* (40), 9070–9079.
- (95) Qin, X.; Pratt, K. A.; Shields, L. G.; Toner, S. M.; Prather, K. A. Seasonal Comparisons of Single-Particle Chemical Mixing State in Riverside, CA. *Atmos. Environ.* **2012**, *59*, 587–596.
- (96) Sullivan, R. C.; Prather, K. A. Investigations of the Diurnal Cycle and Mixing State of Oxalic Acid in Individual Particles in Asian Aerosol Outflow. *Environ. Sci. Technol.* **2007**, *41* (23), 8062–8069.
- (97) Healy, R. M.; Hellebust, S.; Kourtchev, I.; Allanic, A.; O'Connor, I. P.; Bell, J. M.; Healy, D. A.; Sodeau, J. R.; Wenger, J. C. Source Apportionment of PM_{2.5} in Cork Harbour, Ireland Using a Combination of Single Particle Mass Spectrometry and Quantitative Semi-Continuous Measurements. *Atmospheric Chem. Phys.* **2010**, *10* (19), 9593–9613.
- (98) Naeher, L. P.; Brauer, M.; Lipsett, M.; Zelikoff, J. T.; Simpson, C. D.; Koenig, J. Q.; Smith, K. R. Woodsmoke Health Effects: A Review. *Inhal. Toxicol.* **2007**, *19* (1), 67–106.
- (99) García-López, N.; Ingabire, A. S.; Bailis, R.; Eriksson, A. C.; Isaxon, C.; Boman, C. Biomass Cookstove Emissions—a Systematic Review on Aerosol and Particle Properties of Relevance for Health, Climate, and the Environment. *Environ. Res. Lett.* **2025**, *20* (5), 053002.
- (100) Spencer, M. T.; Shields, L. G.; Sodeman, D. A.; Toner, S. M.; Prather, K. A. Comparison of Oil and Fuel Particle Chemical Signatures with Particle Emissions from Heavy and Light Duty Vehicles. *Atmos. Environ.* **2006**, *40* (27), 5224–5235.
- (101) Spencer, M. T.; Prather, K. A. Using ATOFMS to Determine OC/EC Mass Fractions in Particles. *Aerosol Sci. Technol.* **2006**, *40* (8), 585–594.
- (102) Neubauer, K. R.; Johnston, M. V.; Wexler, A. S. Humidity Effects on the Mass Spectra of Single Aerosol Particles. *Atmos. Environ.* **1998**, *32* (14), 2521–2529.
- (103) Brice, B. A.; Swain, M. L. Ultraviolet Absorption Method for the Determination of Polyunsaturated Constituents in Fatty Materials. *JOSA* **1945**, *35* (8), 532–544.
- (104) Zimmermann, R.; Ferge, T.; Gälli, M.; Karlsson, R. Application of Single-Particle Laser Desorption/Ionization Time-of-Flight Mass Spectrometry for Detection of Polycyclic Aromatic Hydrocarbons from Soot Particles Originating from an Industrial Combustion Process. *Rapid Commun. Mass Spectrom.* **2003**, *17* (8), 851–859.

(105) See, S. W.; Balasubramanian, R. Physical Characteristics of Ultrafine Particles Emitted from Different Gas Cooking Methods. *Aerosol Air Qual. Res.* **2006**, *6* (1), 82–92.

(106) Traynor, G. W.; Apte, M. G.; Carruthers, A. R.; Dillworth, J. F.; Grimsrud, D. T.; Gundel, L. A. Indoor Air Pollution Due to Emissions from Wood-Burning Stoves. *Environ. Sci. Technol.* **1987**, *21* (7), 691–697.

(107) May, N. W.; Dixon, C.; Jaffe, D. A. Impact of Wildfire Smoke Events on Indoor Air Quality and Evaluation of a Low-Cost Filtration Method. *Aerosol Air Qual. Res.* **2021**, *21* (7), 210046.

(108) Yu, Y.; Dunne, J. P.; Shevliakova, E.; Ginoux, P.; Malyshev, S.; John, J. G.; Krasting, J. P. *Increased Risk of the 2019 Alaskan July Fires due to Anthropogenic Activity*, 2021.

(109) Schoennagel, T.; Balch, J. K.; Brenkert-Smith, H.; Dennison, P. E.; Harvey, B. J.; Krawchuk, M. A.; Mietkiewicz, N.; Morgan, P.; Moritz, M. A.; Rasker, R.; Turner, M. G.; Whitlock, C. Adapt to More Wildfire in Western North American Forests as Climate Changes. *Proc. Natl. Acad. Sci. U.S.A.* **2017**, *114* (18), 4582–4590.



CAS BIOFINDER DISCOVERY PLATFORM™

PRECISION DATA FOR FASTER DRUG DISCOVERY

CAS BioFinder helps you identify
targets, biomarkers, and pathways

Unlock insights

CAS
A division of the
American Chemical Society